Mobilization Distance for Upheaval Buckling of Shallowly Buried Pipelines

J. Wang[1]; S. K. Haigh[2]; G. Forrest[3]; and N. I. Thusyanthan[4]

Abstract: Buried pipelines may be subject to upheaval buckling because of thermally induced compressive stresses. As the buckling load of a strut decreases with increasing out of straightness, not only the maximum available resistance from the soil cover, but also the movement of the pipeline required to mobilize this are important factors in design. This paper will describe the results of 15 full-scale laboratory tests that have been carried out on pipeline uplift in both sandy and rocky backfills. The cover to diameter ratio ranged from 0.1 to 6. The results show that mobilization distance exhibits a linear relationship with H/D ratio and that the postpeak uplift force-displacement response can be accurately modeled using existing models. A tentative design approach is suggested; the maximum available uplift resistance may be reliably predicted from the postpeak response, and the mobilization distance may be predicted using the relationships described in this paper. **DOI: 10.1061/(ASCE)PS.1949-1204.0000099.** © *2012 American Society of Civil Engineers.*

CE Database subject headings: Soil-structure interactions; Buckling; Uplifting; Design; Buried pipes.

Author keywords: Soil-structure interaction; Upheaval buckling; Uplift resistance; Mobilization distance; Geotechnical; Design.

Introduction

Most onshore and mature offshore oil-producing sites feature heavy usage of small to medium diameter infield pipelines. These pipelines vary in diameter between 100 and 500 mm and are usually buried for additional thermal insulation and for protection from physical damage. This may be from anchor gear and fishing activities offshore and from construction activities or collisions onshore. At present, the preferred installation method for these pipelines is the reel-lay technique, which requires thick-walled pipes to prevent buckling during the bending and straightening process. As this process has to be conducted at the in situ ambient temperature, typically 4°C, thermally induced axial compressive forces can develop during operation as the temperature of the oil passing through these pipelines is typically around 140°C. Given the high degree of lateral and axial soil restraint, these pipelines may be forced upwards out of their burial trench in a phenomenon known as upheaval buckling. The backfill soil above the pipe crown must thus provide vertical resistance to prevent the upheaval of the pipeline.

Upheaval buckling (UHB), like all buckling processes, is very sensitive to the straightness of the pipeline. During the upheaval process, upward movement of the pipeline leads to relief of the axial compressive force in the pipeline, thus reducing the tendency of the pipeline to suffer further displacement. The pipeline curvature, however, increases, making the compression force required for further buckling reduce. The upheaval buckling stability of pipelines is therefore governed not only by the maximum available soil resistance, but also by the displacement of the pipeline that is required to mobilize this resistance. While the maximum net soil downward resistance during the uplift event (R_{peak}) has been widely studied, the equally critical question of the prepeak force-displacement behavior has been less so. This prepeak behavior may be characterized by the upward movement of the pipe required to mobilize the peak downward resistance. This could be termed the mobilization distance (δ_f). This research paper draws its conclusions from a series of full-scale pipeline uplift tests, it aims to provide insights into how mobilization distance affects UHB design and how its value may be predicted based on simple design parameters for upheaval buckling in both sandy and rocky backfills.

Previous Research and Current Practice

The UHB stability of the pipeline is governed by the force balance between the axial compressive force (P) and the available downward restraint (Timoshenko and Goodier 1934). The general solution addressing structural equilibrium is given by Palmer et al. (1990) as being of the form shown in Eq. (1):

$$\Phi_W = A\left(\frac{\pi}{\Phi_L}\right)^2 - B\left(\frac{\pi}{\Phi_L}\right)^4 \tag{1}$$

where $\Phi_W = R(EI/\Delta P^2)$ = dimensionless uplift resistance; $\Phi_L = L(P/EI)^4$ = dimensionless imperfection length; EI = flexural rigidity of the pipeline; P = thermally-generated axial compressive force; Δ = maximum height of the imperfection; L = half the total imperfection length; and A and B = constants to be determined numerically. The solution for any particular pipeline section will

[1]Engineer, Det Norske Veritas UK, Palace House, 3 Cathedral St., London, UK, SE1 9DE; formerly, Schofield Centre, Univ. of Cambridge (corresponding author). E-mail: junkan.wang@gmail.com

[2]Lecturer, Schofield Centre, Univ. of Cambridge, High Cross, Madingley Rd., Cambridge, Cambridgeshire, UK, CB3 0EL. E-mail: skh20@cam.ac.uk

[3]Senior Project Engineer, Babcock International Group, Devonport Royal Dockyard, Plymouth, UK, PL1 4SG. E-mail: graham.forrest@cantab.net

[4]Engineering Manager, Cape Group Pte Ltd., 35 Pioneer Rd., #03-09, Singapore, 628503; formerly, KW Ltd. E-mail: thusyanthan@capegroup.net

Note. This manuscript was submitted on April 26, 2011; approved on November 21, 2011; published online on November 23, 2011. Discussion period open until April 1, 2013; separate discussions must be submitted for individual papers. This paper is part of the ***Journal of Pipeline Systems Engineering and Practice***, Vol. 3, No. 4, November 1, 2012. © ASCE, ISSN 1949-1190/2012/4-106-114/$25.00.

depend on the initial imperfection profile (Croll 1997). As Φ_w intrinsically depends upon Δ, any additional upward movement of the pipeline would act as feedback into calculation.

The breakout resistance of objects embedded in soil consists of four general components (Vesic 1971): (1) submerged effective weight of the object; (2) submerged effective weight of soil being lifted; (3) vertical component of the soil shearing resistance; and (4) vertical component of the suction force from excess pore pressure differences above and below the object. For pipeline UHB design, the soil resistance to uplift (R) is often defined as the aggregate of the second and the third components only. Bransby and Ireland (2009) showed that this definition was conservative in cohesionless soils, in that increased pullout speed resulted in higher recorded uplift force from higher negative pore pressure being generated underneath the pipe.

The current prediction method for R_{peak} has evolved from the vertical slip-surface model developed by Schaminée et al. (1990), as shown in Fig. 1(a). This assumes that the resistance to upheaval buckling is derived from both the weight of soil above the pipeline and from shear stresses on vertical shear planes originating from the sides of the pipe and propagating to the backfill soil surface. The parameter (K) in this figure is the lateral effective earth pressure coefficient and is a function of the soil intergranular friction angle (ϕ) only. In cohesionless backfills, the assumption that shear strength is directly proportional to vertical effective stress implies that the maximum available soil resistance to uplift (R_{peak}) can be expressed in the form of Eq. (2). This design equation has been implemented into the design code DNV [Det Norske Veritas (DNV) 2007] with guideline design values for f_p being summarized in Table 1.

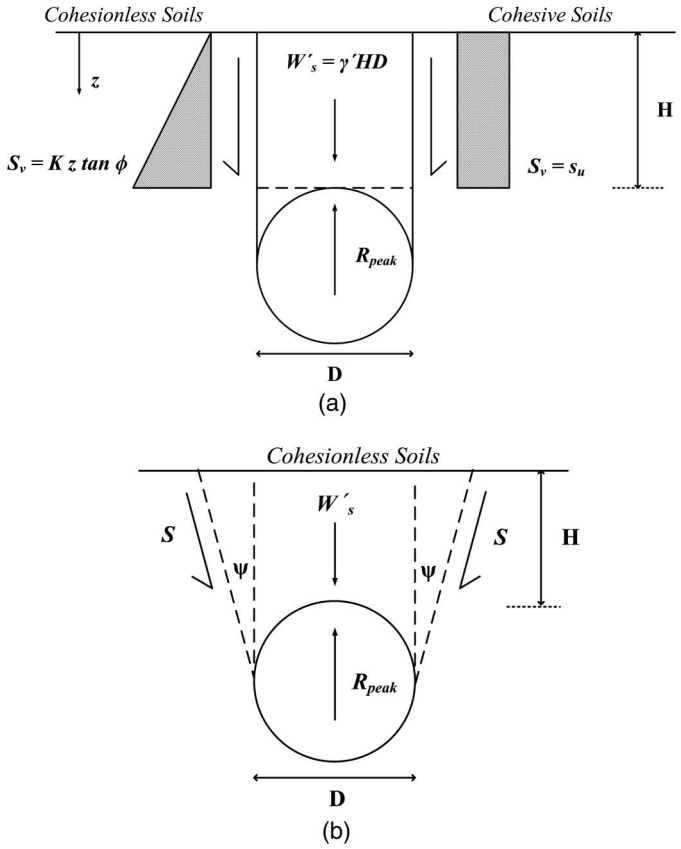

Fig. 1. Proposed soil resistance models at R_{peak}: (a) vertical slip-surface model; (b) inclined slip-surface model

Table 1. Recommended Values for f_p (DNV 2007)

Backfill type	ϕ_{peak} (°)	H/D range	Mean f_p	Range of f_p
Loose sand	30	[3.5, 7.5]	0.29	[0.1, 0.3]
Medium sand	35	[2.0, 8.0]	0.47	[0.4, 0.6]
Dense sand	40	[2.0, 8.0]	0.62	
Rock	N/A	[2.0, 8.0]	0.62	[0.5, 0.8]

$$\frac{R_{\text{peak}}}{\gamma' HD} = 1 + \left(0.5 - \frac{\pi}{8}\right)\frac{D}{H} + f_p\left[\frac{D}{H} \times \left(\frac{H}{D} + 0.5\right)^2\right] \tag{2}$$

An alternative, simplified expression proposed by Schaminée et al. (1990) is of the form of Eq. (3), where, H_c = height of soil above the pipe centerline. This simplified form is only an approximation and can only be adopted for design scenarios with medium to large H/D ratios. For analytical accuracy, Eq. (2) will be adopted throughout this paper:

$$\frac{R_{\text{peak}}}{\gamma' HD} = 1 + f\frac{H_s}{D} = 1 + f\frac{H + 0.5D}{D} \tag{3}$$

Recent experimental evidence based on soil imaging techniques (Wang et al. 2010a), reveals that the vertical slip-surface model is only approximate for uplift in loose sand at medium H/D ratios. For uplift in medium to dense sands, the deformation mechanism exhibits similarity with the inclined slip-surface model, (White et al. 2001), featuring inclined symmetrical slip planes with the angle of inclination equal to the angle of dilatancy (ψ) of the sand in shear, as shown in Fig. 1(b). A similar mechanism is also observed for uplift in loose sand at low H/D ratios (H/D <1). By assuming the normal effective stress perpendicular to the shear planes remains constant during the uplift event, R_{peak} can be expressed in terms of purely physical parameters [Eq. (4)]:

$$\frac{R_{\text{peak}}}{\gamma' HD} = 1 + \left(0.5 - \frac{\pi}{8}\right)\frac{D}{H} + \left\{\tan\psi + \frac{1}{2}(\tan\phi_{\text{peak}} - \tan\psi) \times [(1 + K_0) - (1 - K_0)\cos 2\psi]\right\} \times \left[\frac{D}{H} \times \left(\frac{H}{D} + 0.5\right)^2\right] \tag{4}$$

The similarity between Eqs. (2) and (4) should be noted. It seems that the form of Eq. (2) is not sensitive to the particular shallow failure mechanism chosen. Hence, it may be regarded as a universally applicable expression for R_{peak} in sandy backfills at low to medium H/D ratios.

Experimental data from previous research (Trautmann et al. 1985; Schaminée et al. 1990; Baumgard 2000; Palmer et al. 2003; Wang et al. 2010a) supports the hypothesis that the value of f_p remains reasonably constant for a particular pipe geometry and backfill condition. This assumption breaks down, however, when a deep flow-around type mechanism begins to occur, typically beyond $H/D = 6$.

While prediction of R_{peak} is rather well established, relatively little research effort has hitherto been devoted to a prediction method for the corresponding pipe upward displacement (δ_f) required to achieve this maximum "true" uplift resistance. One underlying reason for this is the scaling law discrepancy for mobilization distance between small-scale centrifuge and full-scale test data. Previous research (Palmer et al. 2003) confirmed that, while centrifuge modeling offers reasonably accurate estimates for R_{peak}, the standard distance scaling law could not be used to derive δ_f

J. Pipeline Syst. Eng. Pract., 2012, 3(4): 106-114

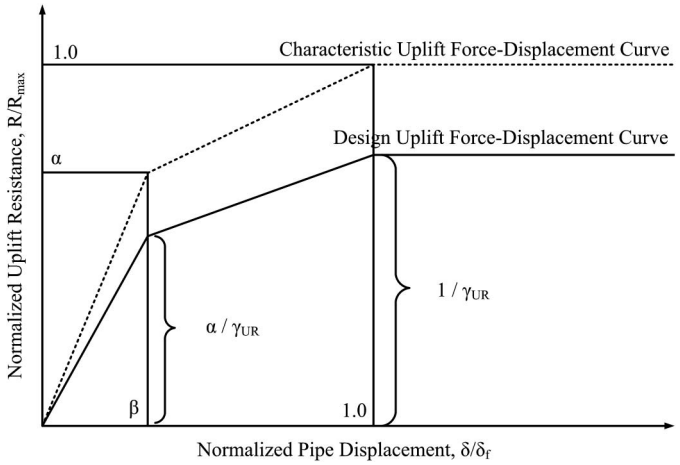

Fig. 2. Trilinear uplift force-displacement model with global safety factor applied

Table 2. Parameters for DNV Trilinear Design Curve

Soil type	Parameter		Range
Loose sand	δ_f	ϵ	[0.5%, 0.8%] H
(H/D range 3.5 to 7.5)	α	ϵ	[0.75, 0.85]
	β	=	0.2
Medium/Dense sand	δ_f	ϵ	[0.5%, 0.8%] H
(prepeak) (H/D range 2 to 8)	α	ϵ	[0.65, 0.75]
	β	=	0.2
Rock (H/D range 2 to 8)	δ_f	ϵ	[20 mm, 30 mm]
	α	ϵ	0.35 D
	β	=	0.2

because of localized shear zone formation. As the thickness of the shear zone is a multiple of the particle diameter, the pipeline movement required to mobilize full uplift resistance is a function of the ratio of the diameters of the pipe and the soil particles. This has limited the volume of data available for the prediction of mobilization distance, as a sizeable proportion of the available data is from small-scale centrifuge model testing.

The current prediction method for δ_f is based on the normalized trilinear uplift force-displacement curve shown in Fig. 2. The global safety factor (γ_{UR}) is also included for completeness. The geometry of this trilinear characteristic curve can be defined by three parameters: α, β, and δ_f. The ranges of these parameters prescribed by DNV (2007) for different types of cohesionless backfill are summarized in Table 2. A few observations can be made:

- For sandy backfills, δ_f is normalized with H; the δ_f/H values are independent of the H/D ratio; and
- For rocky backfills, δ_f is not normalized.

The experimental data from which these guidelines have been derived is not explicitly stated in the design code.

Experimental Program

A comprehensive series of pipeline uplift resistance tests in sandy and rocky backfills have been carried out. All tests were conducted at full scale, acknowledging the known issue with scaling of δ_f from centrifuge testing. The series can be subdivided into the following categories:

I. Plane-strain testing in loose, fully saturated Fraction E sand using a 100-mm-diameter model pipe;
II. Plane-strain testing in loose, fully saturated Fraction E sand using a 258-mm-diameter model pipe;
III. Plane-strain testing in dry gravel ($D_{50} = 5$ mm approx.) using a 100-mm-diameter model pipe; and
IV. Plane-strain testing in dry gravel ($D_{50} = 5$ mm approx.) using a 160-mm-diameter model pipe.

Fraction E sand is a clean, well-graded, subangular laboratory sand commonly used for geotechnical physical modeling tests. Its material properties and particle size distribution resemble soil samples from many near-shore seabed sites. It was prepared at a relative density $I_D = 35\%$ giving a saturated unit weight γ_{sat} of 18.5 kN/m^3. The dry gravel used in these tests is quarried and is slightly smaller than that used in offshore rock dumping on top of backfilled pipelines for UHB prevention. The particle size distributions obtained by the single-particle optical sizing (SPOS) method for the two soils are shown in Fig. 3. It should be noted that the SPOS method picks up the largest dimension of soil grains, and hence particle size values obtained from this method tend to exceed traditional sieving data (White 2003). The effect of particle angularity on the experimental results remains to be investigated.

As the focus of these experiments was soil-structure interaction, it was appropriate, at this stage, to eliminate the influence of structural deformation on the experimental results. Hence, thick-walled model pipes were used which could be deemed to be rigid for the range of uplift load concerned in all these experiments. In real design scenarios, pipeline ring stiffness must be taken into account as any deformation of the pipe cross section would lead to an increase in the movement of the pipe center required to mobilize full resistance. The model pipes' outer surfaces were either aluminium or HDPE, so a smooth pipe-soil interface could be assumed. This represented the worst-case design scenario in UHB as the shear contribution from interface friction was minimized.

The plane strain testing setup and procedures for uplift in sandy backfills are described in detail by Wang et al. (2010b). A schematic of the test tank is shown in Fig. 4. The container has internal dimensions of 1,000 mm (length) × 76 mm (width) × 850 mm (height). Its front face comprises of a 25 mm thick Perspex sheet that enables usage of the particle image velocimetry (PIV) technique so that the displacement field of the backfill can be measured throughout the pullout event. The pipeline uplift was displacement controlled at a rate of 0.005 mm/s. A pore pressure transducer (PPT) was embedded in the bottom of the model pipes. During all tests in Categories I and II, very small negative excess

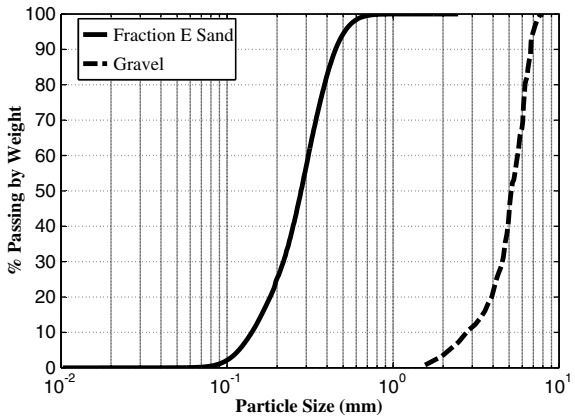

Fig. 3. Particle size distribution (PSD) curves for fraction *E* sand and gravel

J. Pipeline Syst. Eng. Pract., 2012, 3(4): 106-114

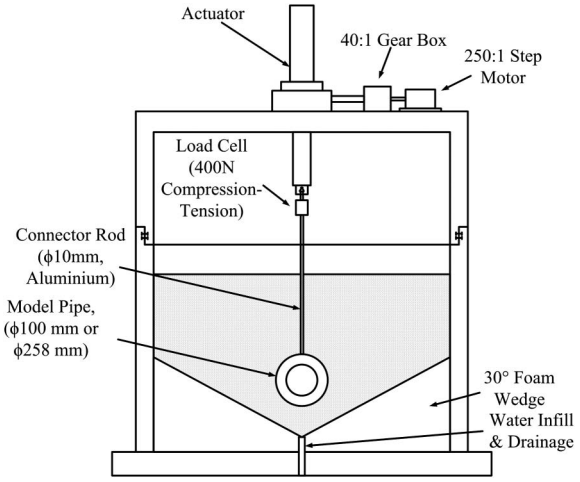

Fig. 4. Full-scale plane-strain tank for uplift testing in sandy backfills

pore pressures (<20 Pa) were observed, i.e., drained conditions were achieved.

The test setup for uplift in rocky backfills is shown schematically in Fig. 5. The test tank has internal dimensions 500 mm (length) × 1,490 mm (width) × 895 mm (height). Two model pipes were used, each of total effective length 494 mm, with external diameters of 100 mm and 160 mm. Both model pipes had smooth PTFE ends that were in close contact with 3-mm-thick PTFE sheets glued to the inside of the container. All PTFE surfaces were repolished and greased before each test so that frictional end effects were minimized. Two 10-mm-diameter threaded aluminium rods attached the pipe section to the actuator. The cross-sectional area of these rods accounted for less than 0.4% of the projected total area of the pipe; hence, their influence on the test results could be ignored. The uplift movement was provided by an electric winch, which was connected to the load cell via a 5-mm-diameter steel wire. The nature of the winch meant that the greater the cover depth, the slower the pull-up speed. Hence, it was not possible to conduct strict strain-controlled testing. However, as the backfill was dry gravel and the maximum pull-up speed was below 10 mm/s, it would not be expected to observe any significant rate effects on the soil resistance.

Fifteen tests were conducted across all four categories. The full test program is summarized in Table 3.

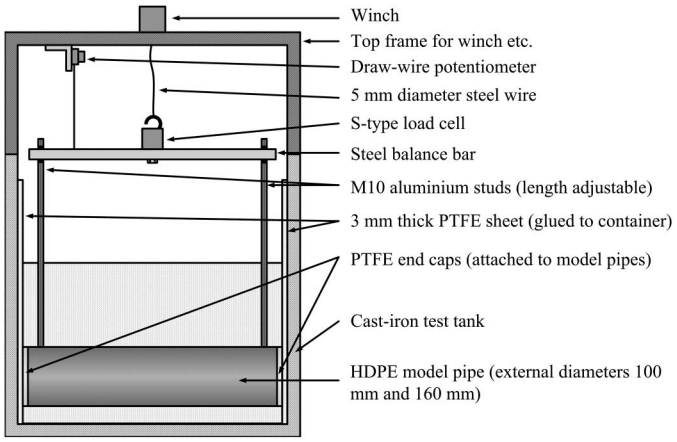

Fig. 5. Full-scale tank for uplift testing in rocky backfills

Table 3. Test Program Summary

Test number	Category	Backfill	D_{50} (mm)	γ_{dry} (kN/m^3)	γ_{sat} (kN/m^3)	D (mm)	H (mm)
1	I	Saturated	0.28	14.1	18.5	100	10
2		Fraction		(±1.0%)	(±1.0%)		50
3		E sand					100
4							200
5							350
6	II					258	110
7							129
8							258
9	III	Dry	6	13.7	N/A	100	400
10		gravel		(±0.5%)			500
11							600
12	IV					160	80
13							160
14							320
15							480

Test Results

Fig. 6 shows the recorded uplift force per unit pipe length against pipe upward displacement for all tests. The recorded mobilization distance and back-calculated f_p values are shown in Table 4. As most of the curves feature either flat or multiple peaks, particularly at low H/D ratios, the precise movement required to mobilize full displacement is quite uncertain. Given that a global safety factor is often applied to peak loads in design, more applicable values for mobilization distance could be defined as the upward pipeline displacement required to mobilize a certain fraction of R_{peak}. As the global safety factor varies from case to case, a number of possible thresholds have been investigated: 60, 70, 80, 90, and 95% of R_{peak}. Mobilization distances corresponding to these thresholds are tabulated in Table 4.

Analysis and Discussion

Prepeak Behavior

In the prediction of upheaval buckling, the mobilization distance is a function of cover depth (H), pipe diameter (D), the backfill mean particle size (D_{50}), the critical-state interparticle friction angle (ϕ_{crit}) and the soil dilation angle (ψ). By dimensional analysis, the relationship shown in Eq. (5) must hold:

$$\frac{\delta_f}{D} = f\left(\frac{H}{D}, \frac{D}{D_{50}}, \phi_{crit}, \psi\right) \tag{5}$$

δ_f could also be normalized by H or D_{50}, and the resulting equation would be equally valid. The preferred method of normalization should depend on design convenience. The current design method (DNV 2007) suggests that, for upheaval buckling in sandy backfills, normalizing mobilization distance with H should give values of between 0.5 and 0.8%, and the value should be independent of the H/D ratio, while for upheaval buckling in rocky backfills, mobilization distance is not normalized and is deemed to simply fall between 20 and 30 mm.

Fig. 7 plots the recorded actual mobilization distance against H/D ratios for all rock test data. Fig. 8 plots the normalized δ_f/H values against H/D ratios for all tests except Test 1, where the H value is too small for normalization. It is evident that the test results obtained do not support the current design method. Recorded δ_f/H values from tests with sandy backfills universally

J. Pipeline Syst. Eng. Pract., 2012, 3(4): 106-114

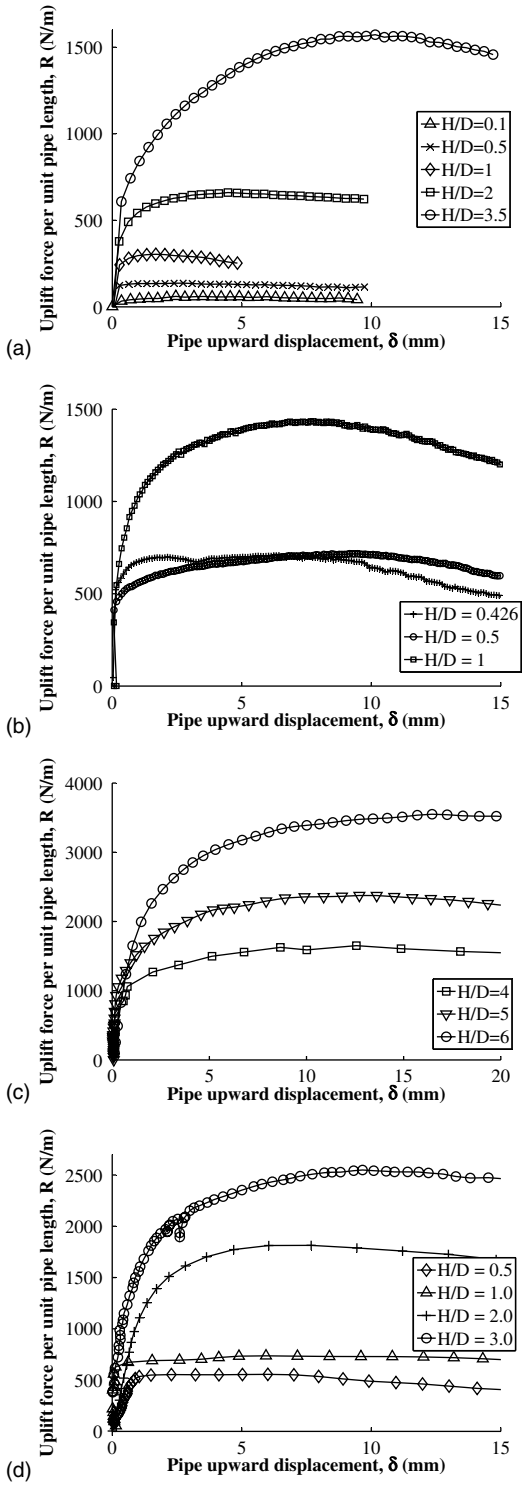

Fig. 6. Uplift force-displacement curves for all tests, grouped according to category

exceed the suggested 0.8% upper threshold, whereas all recorded δ_f values from tests with rocky backfills undershoot the suggested 20 mm lower threshold.

Fig. 8 illustrates that, despite the significant difference in backfill D_{50} values between the two backfills, similar normalized mobilization distances are measured, which suggests that Eq. (5) may be further simplified to the form of Eq. (6). This simplification is consistent with previous research findings that δ_f is insensitive to particle size effects. It is worth pointing out that such insensitivity is not inconsistent with the known problem that δ_f does not scale conventionally in centrifuge tests. Palmer et al. (2003) suggested that this could be tentatively explained as a result of localized shear stress being a function of relative absolute displacement:

$$\frac{\delta_f}{D} = f\left(\frac{H}{D}, \phi_{\text{crit}}, \psi\right) \tag{6}$$

The variation in ϕ_{crit} for common cohesionless backfill soils is small, between 30° and 40° for most onshore and offshore applications (Terzaghi et al. 1996). Its influence on the macroscopic δ_f may thus be small. Furthermore, particularly in offshore conditions, the trenching depth is largely limited by cost and the available ploughing capacity. It is hence very unusual for H to exceed 3 m. This implies that the average mean principle effective stress (p') in upheaval buckling design is normally below 30 kPa. Under such low effective stresses, the backfill soils would almost always have a tendency to dilate during plane-strain shear unless the backfill relative density (I_D) is below 10%. For realistic loose sandy and rocky backfill conditions, (I_D between 25% and 35%), the angle of dilatancy (ψ) could be estimated using the stress-dilatancy approximations of Bolton (1986) as being between 3° and 8°. For medium, dense, or compacted backfills, the angle of dilation may be as high as 20° and its influence on δ_f might be significant.

Based on the data shown above, for the H/D ratios tested ($0 < H/D < 6$) conservative estimates for the lower and upper bounds on the δ_f/H values in loose cohesionless backfills may be defined using Eq. (7). In the range of H/D ratios commonly used, between 2 and 5, this range may be further narrowed using Eq. (8):

$$\frac{\delta_f}{H} \in [1\%, 8\%] \quad \left(0 < \frac{H}{D} < 6\right) \tag{7}$$

$$\frac{\delta_f}{H} \in [1.5\%, 4.5\%] \quad \left(2 < \frac{H}{D} < 5\right) \tag{8}$$

It is very difficult to determine a credible value for normalized mobilization distance that is applicable across the entire H/D range tested. The narrow ranges at medium H/D ratios are from the easily identifiable and relatively narrow peaks in the force-displacement curves under laboratory conditions. At lower and higher H/D ratios, the curves are much flatter and peaks are harder to define resulting in a greater scatter in the results. At high H/D ratios, a deep flow-around mechanism will start to dominate and mobilization distance may no longer be a linear function of H. This correlation between δ_f/H and H/D ratios should thus not be extrapolated beyond the H/D range and backfill conditions for which it has been derived.

As mentioned previously, the use of factors of safety on peak load in design implies that the pipe movement required to mobilize a fraction of the uplift resistance may be important. Fig. 9 shows the variation in mobilization distances normalized by pipe diameter against H/D. The graph also shows the normalized pipe movements corresponding to 60, 70, 80, 90, and 95% of peak uplift resistance.

It can be seen that at every threshold level, the recorded δ/D values seem to vary linearly with H/D ratio according to the generalized form shown in Eq. (9):

$$\frac{\delta_f}{D} = M \times \frac{H}{D} + N \tag{9}$$

Table 4. Summary of Recorded δ_f Values and Back-Calculated f_p Values for All Tests

Test number	Category	H/D	R_{peak} (kN/m)	f_p	δ_f (mm)	δ at 60% R_{peak} (mm)	δ at 70% R_{peak} (mm)	δ at 80% R_{peak} (mm)	δ at 90% R_{peak} (mm)	δ at 95% R_{peak} (mm)
1	I	0.1	63.1	1.4	3.3	0.59	0.96	1.60	2.12	2.43
2		0.5	139	0.99	2.5	0.08	0.13	0.20	0.23	0.42
3		1	306	1.1	1.7	0.09	0.15	0.29	0.45	0.72
4		2	663	0.88	4.5	0.31	0.51	0.87	1.52	2.32
5		3.5	1,580	0.91	10	1.51	2.38	3.65	5.21	6.57
6	II	0.426	710	0.81	6.4	0.06	0.10	0.27	0.61	1.02
7		0.5	722	0.64	9.7	0.10	0.40	1.30	3.45	5.67
8		1	1,440	0.61	7.7	0.58	0.95	1.65	3.02	4.48
9	III	4	1,670	0.40	14	0.94	1.43	2.83	5.26	7.49
10		5	2,380	0.40	13	1.05	1.76	3.09	4.95	7.37
11		6	3,550	0.47	17	1.80	2.72	4.14	6.97	9.49
12	IV	0.5	555	0.98	6.0	0.52	0.60	0.68	0.85	1.00
13		1	737	0.44	5.7	0.07	0.07	0.07	0.48	3.30
14		2	1,820	0.49	7.0	1.06	1.41	1.98	3.13	4.03
15		3	2,550	0.34	9.6	0.96	1.46	2.32	4.37	5.96

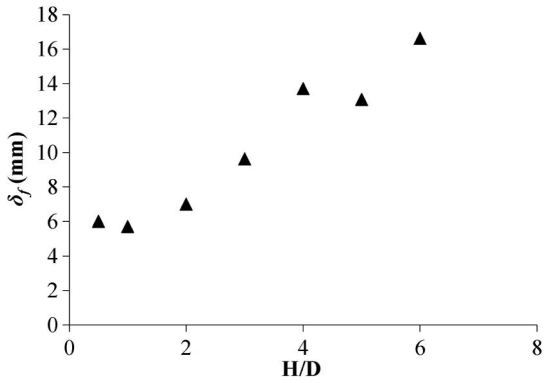

Fig. 7. Plot of δ_f values against H/D ratios for gravel tests

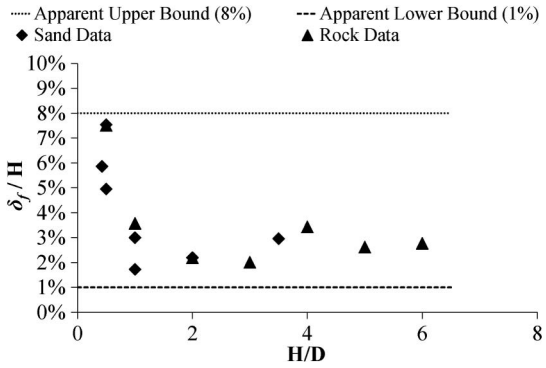

Fig. 8. Plot of δ_f/H values against H/D ratios for tests 2 to 15

The gradient M gradually increases as the threshold level is increased. The values for M and N across different thresholds are tabulated in Table 5. The best fit trend lines all have small offsets on the δ/D axis. The quality of these correlations is quite satisfactory, with R^2 values of between 0.84 and 0.93. The nonzero intercepts of these trend lines on the δ/D axis indicate slight deviations in shapes of R/R_{peak} versus δ/δ_f curves with varying H/D ratio.

Based on these trend lines, curves for normalized load R/R_{peak} versus normalized displacement δ/δ_f can be derived and compared with the current DNV guidelines (Fig. 10). It is clear that if δ_f values can be correctly predicted, the current lower-bound trilinear curve does lead to conservative design for prepeak R-δ behavior.

Postpeak Behavior

The pipe movements for tests in Categories III and IV (tests 9 to 15) were sufficiently large for the postpeak R-δ response to be examined. The traditional assumption is that loose sandy backfills will exhibit contractile behavior in shearing during the uplift event, and hence R-δ curves should exhibit a rather flat "plateau." However, as the confining effective stresses in upheaval buckling design scenarios are low, even loose sands (I_D between 25% and 35%) will tend to dilate with ψ values between 5° and 8°. Hence, the resulting postpeak R-δ should still be somewhat "brittle."

For cohesionless soils in general, as the backfill continues to shear as uplift progresses, a critical state will be reached when ψ reaches 0° (Schofield and Wroth 1968). By ignoring heave of the backfill surface and assuming that Eq. (2) is still insensitive to the postpeak mechanism, it can be argued that, after the critical state is reached, R at any instant during the uplift event may be expressed as a function of the remaining cover on top of the pipe crown. The resulting uplift resistance [Eq. (10)] would hence be very similar to Eq. (2) with H replaced with $(H_0 - \delta)$ and f_p replaced by f_r (indicating the "residual" uplift factor). At critical state, f_r should be independent of the pipe geometry, being purely a function of ϕ_{crit} (the postpeak lateral effective earth pressure coefficient K is also solely a function of ϕ_{crit}):

$$\frac{R}{\gamma'(H_0-\delta)D} = 1 + \left(0.5 - \frac{\pi}{8}\right)\frac{D}{(H_0-\delta)} + f_r\left[\frac{D}{(H_0-\delta)} \times \left(\frac{(H_0-\delta)}{D} + 0.5\right)^2\right] \quad (10)$$

A convenient way to examine the validity of Eq. (10) is to plot R against $(\delta - H_0)$ for all tests within the same category. If the postpeak critical-state assumptions are true, then the postpeak segments of all these curves should tend to an underlying "backbone" trend line. This is shown in Fig. 11.

The tests shown in Fig. 11 were conducted in rocky backfill. The small ratio between the pipe cover and the particle size can result in fluctuations in uplift responses from particle interlocking. However, the load-displacement curves in each category still tended to a single backbone trend line consistent with Eq. (10), and the correlation is rather satisfactory. A common f_r value of

J. Pipeline Syst. Eng. Pract., 2012, 3(4): 106-114

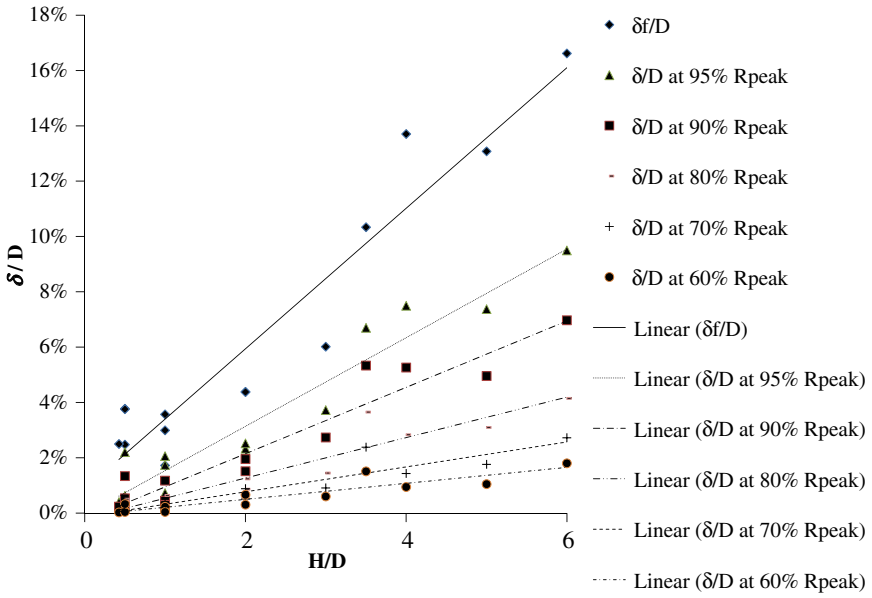

Fig. 9. Plot of δ_f/D values against H/D ratios for tests 2 to 15 with best fit trend lines

Table 5. Trend Line Predictions for δ at Various Thresholds of R_{peak}

Threshold (% R_{peak})	M	N (%)	R^2
60	0.003	−0.08	0.84
70	0.004	−0.1	0.86
80	0.007	−0.2	0.90
90	0.012	−0.3	0.92
95	0.016	−0.07	0.93
100	0.025	+0.9	0.91

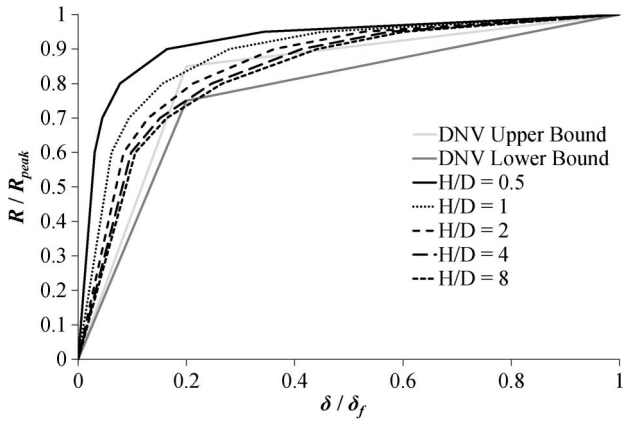

Fig. 10. Suggested curves of R/R_{peak} against δ/δ_f based on best fit trend lines and DNV guidelines

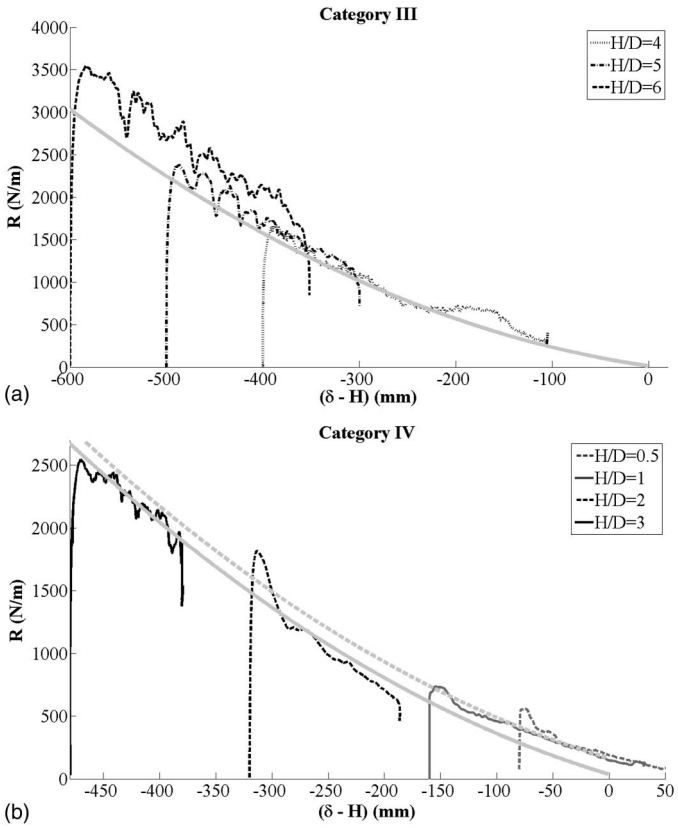

Fig. 11. Plot of R against $(\delta - H_0)$ for tests within (a) category III; (b) category IV with trend lines fitted according to Eq. (10)

0.38 was applicable in both plots, verifying the fact that f_r is independent of pipe geometry and is a function of backfill soil properties only.

At relatively low H/D ratios (≤1), the assumption of no heave at the backfill surface is not strictly true, as a triangular or trapezoidal soil wedge forms after a little post-peak pipe displacement, illustrated in Fig. 12. The shape of the wedges tends to be rather stable, with slope angles equal to ϕ_{crit} and a base length approximately 1.5 times the pipe diameter D. Hence an extra term, shown in Eq. (11), should be added to the resulting R value to represent the additional weight of this wedge:

$$W_{wedge} = \frac{\gamma' D^2}{2} \tan \phi_{crit} \tag{11}$$

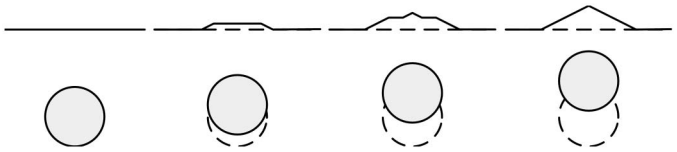

Fig. 12. Schematic soil wedge formation at surface (approximate) at low H/D ratios

This adjustment is applied to the original trend line in Fig. 11(b), with the resulting dashed line being seen to fit the test data at $H/D = 0.5$ and 1 very well, but overshooting at higher H/D ratios. From a design perspective, it would be reasonable to ignore the W_{wedge} component of resistance completely, the resulting predictions based on Eq. (10) being conservative and widely applicable.

It could be argued that f_r is inherently more reliable than f_p in that it is based on the critical-state strength rather than the peak strength of the soil and is hence free from any influence of brittleness from dilation. For reliable conservative design against upheaval buckling, it is hence advised that the designer should resort to the underlying postpeak backbone curve to derive a best-fit value for f_r, and use this number to derive a safe prediction for R_{peak}.

Conclusions

This research draws conclusions from 15 full-scale laboratory tests on pipeline uplift resistance. The results indicate that, at shallow burial depth (≤0.6 m), mobilization distance may be predicted by assuming a linear relationship between δ/D and H/D using Eq. (9) and the data in Table 5, this relationship being applicable in both loose sands and gravels. This mobilization distance may significantly exceed that currently suggested by DNV (2007), and the latter could potentially result in nonconservative designs.

The results also suggest that the post-peak uplift force-displacement response may be accurately predicted based on Eq. (10) and a residual uplift factor (f_r). Experimental evidence suggests that f_r is a critical-state parameter and depends only on ϕ_{crit} of the backfill. Hence, f_r could offer a more conservative, consistent and reliable prediction of the maximum available uplift resistance than the recorded peak approach.

Based on these findings, the following approach is tentatively suggested for upheaval buckling design in loose sandy and rocky backfills with cover depth not exceeding 0.6 m:

1. Derive a reliable estimate for f_r based on either experimental data or geotechnical parameters (K and ϕ_{crit});
2. Use Eq. (9) and the data in Table 5 to estimate the prepeak normalized uplift force-displacement behavior;
3. Combine 1 and 2 to produce a characteristic pipeline uplift force-displacement curve applicable for pre-peak upward displacements of the pipeline; and
4. Apply a safety factor consistent with, for example, DNV (2007), to produce a corresponding design force-displacement curve.

Acknowledgments

The authors would like to thank KW Limited for its generous financial and informational support towards the completion of this research. The first author would also like to thank Trinity College, University of Cambridge for funding his Ph.D. research on this subject.

Notation

The following symbols are used in this paper:

D = pipe external diameter [L];
f = simplified uplift factor [-];
f_p = DNV uplift factor at peak uplift resistance [-];
f_r = postpeak residual uplift factor [-];
H = depth of soil cover measured from soil surface to pipe crown [L];
H_c = depth of soil cover measured from soil surface to pipe center [L];
H_0 = initial depth of soil cover measured from soil surface to pipe crown [L];
K = lateral effective earth pressure coefficient [-];
K_0 = insitu lateral effective earth pressure coefficient [-];
R = net soil downward resistance to UHB per unit pipe length [MT^{-2}];
R^2 = statistical measure of how wellregression line approximates real data points [-];
S_v = vertical component of soil shear resistance to UHB per unit pipe length [MT^{-2}];
s_u = undrained shear strength for clays [$ML^{-1}T^{-2}$];
z = depth measured from soil surface [L];
α = DNV trilinear design curve coefficient [-];
β = DNV trilinear design curve coefficient [-];
γ' = submerged soil unit weight [$ML^{-2}T^{-2}$];
γ_{UR} = DNV global safety factor [-];
δ = upward pipe displacement or mobilization distance [L];
δ_f = upward pipe displacement or mobilization distance at peak uplift resistance [L];
ϕ_{crit} = critical-state soil intergranular friction angle [-]; and
ψ = angle of dilation for granular soils in shear [-].

References

Baumgard, A. J. (2000). "Monotonic and cyclic soil responses to upheaval buckling in offshore buried pipelines." Ph.D. thesis, Univ. of Cambridge, UK.

Bolton, M. D. (1986). "The strength and dilatancy of sands." *Géotechnique*, 36(1), 65–78.

Bransby, M. F., and Ireland, J. (2009). "Rate effects during pipeline upheaval buckling in sand." *Geotech. Eng.*, 162(5), 247–256.

Croll, J. G. (1997). "A simplified model of upheaval thermal buckling of subsea pipelines." *Thin-Walled Struct.*, 29(1–4), 59–78.

Det Norske Veritas (DNV). (2007). "Global buckling of submarine pipelines—Structural design due to high temperature/high pressure." *DNV-RP-F110*, Det Norske Veritas, Baerum, Norway.

Palmer, A. C. (2003). "Uplift resistance of buried submarine pipelines: Comparison between centrifuge modelling and full-scale tests." *Géotechnique*, 53(10), 877–883.

Palmer, A. C., Ellinas, C. P., Richards, D. M., and Guijt, J. (1990). "Design of submarine pipelines against upheaval buckling." *Proc., Offshore Technol. Conf.*, 6335-MS, Offshore Technology Conference, Houston, 551–560.

Schaminée, P., Zorn, N., and Schotman, G. (1990). "Soil response for pipeline upheaval buckling analyses: Full-scale laboratory tests and modelling." *Proc. Offshore Technol. Conf.*, Offshore Technology Conference, Houston, 563–572.

Schofield, A., and Wroth, P. (1968). *Critical state soil mechanics*, McGraw-Hill, New York.

Terzaghi, K., Peck, B. R., and Mesri, G. (1996). *Soil mechanics in engineering practice*, 3 Ed., Wiley, London.
Timoshenko, S., and Goodier, J. N. (1934). *Theory of elasticity*, McGraw-Hill, New York.
Trautmann, C. H., O'Rourke, T. D., and Kulhawy, F. H. (1985). "Uplift force-displacement response of buried pipe." *J. Geotech. Eng.*, 111(9), 1061–1076.
Vesic, A. S. (1971). "Breakout resistance of objects embedded in ocean bottom." *J. Soil Mechanics Found. Div.*, 97(9), 1183–1205.
Wang, J., Ahmed, R., Haigh, S. K., Thusyanthan, N. I., and Mesmar, S. (2010a). "Uplift resistance of buried pipelines at low cover-diameter ratios." *Proc. Offshore Technol. Conf.*, OTC-2010-20912, Offshore Technology Conference, Houston.
Wang, J., Haigh, S. K., Thusyanthan, N. I., and Mesmar, S. (2010b). "Mobilisation distance in uplfit resistance modeling of pipelines." *2nd Int. Symp. on Frontiers in Offshore Geotechnics (ISFOG)*, Taylor and Francis, Perth, Australia, 839–844.
White, D. J. (2003). "PSD measurement using the single particle optical sizing (SPOS) method." *Géotechnique*, 53(3), 317–326.
White, D. J., Barefoot, A. J., and Bolton, M. D. (2001). "Centrifuge modelling of upheaval buckling in sand." *Int. J. Phys. Modell. Geotech.*, 1(2), 19–28.